PLOS ONE

RESEARCH ARTICLE

Tris inhibits a GH1 β-glucosidase by a linear mixed inhibition mechanism

Rafael S. Chagas, Sandro R. Marana*

Departamento de Bioquímica, Instituto de Química, Universidade de São Paulo, São Paulo, SP, Brazil

* srmarana@iq.usp.br

Abstract

Here we demonstrate that Tris (2-amino-2-(hydroxymethyl)-1,3-propanediol), largely used as a buffering agent, is a linear mixed inhibitor (K_i = 12 ± 2 mM and α = 3 ± 1) of the GH1 β-glucosidase from the insect *Spodoptera frugiperda* (Sfβgly). Such an inhibition mechanism implies the formation of a non-productive ESI complex involving Sfβgly, substrate, and Tris. In addition, Tris binding reduces by 3 fold the enzyme affinity for the substrate. Hence, at concentrations higher than the K_i, Tris can completely abolish Sfβgly activity, whereas even at lower concentrations the presence of Tris causes underestimation of β-glucosidase kinetic parameters (K_m and k_{cat}). In agreement with the inhibition mechanism, computational docking showed that Tris could bind to a pocket placed at the lateral of the active site opening in the Sfβgly-substrate complex, hence leading to the formation of an ESI complex. In agreement with the crystallographic data available, computational docking also showed that Tris may find binding spots in the interior of the active site of the Sfβgly and several GH1 β-glucosidases. Moreover, the variety of their active site shapes results in a multiplicity of binding profiles, foreseeing different inhibition mechanisms. Thus, Tris inhibition may affect other GH1 β-glucosidases. This remark should be taken into account in their study, highlighting the importance of the appropriate buffer for accurate enzyme characterization.

Citation: Chagas RS, Marana SR (2025) Tris inhibits a GH1 β-glucosidase by a linear mixed inhibition mechanism. PLoS ONE 20(3): e0320120. https://doi.org/10.1371/journal.pone.0320120

Editor: Chenyu Du, University of Huddersfield, UNITED KINGDOM OF GREAT BRITAIN AND NORTHERN IRELAND

Received: November 8, 2024

Accepted: February 13, 2025

Published: March 25, 2025

Data availability statement: All relevant data are within the manuscript and its Supporting information files.

Funding: This project was supported by FAPESP (Fundação de Amparo à Pesquisa do Estado de São Paulo; Grants 2021/03967-6 and 2021/10577-0), CAPES (Coordenação de Aperfeiçoamento de Pessoal de Nível Superior) and CNPq (Conselho Nacional de

1. Introduction

Glycoside hydrolases (GH) are enzymes found in all living forms. Based on their sequence and structural similarities, GH enzymes are categorized into 189 families in the CAZY databank (http://www.cazy.org) [1]. The GH1 family includes β-glucosidases (EC 3.2.1.21) which catalyze the hydrolysis of O- or S-glycosidic linkages of β-glycosides, playing important functions in numerous biological processes [2].

The GH1 β-glucosidases present a $(\beta/\alpha)_8$ barrel fold in which the active site is placed among the loops projecting from the C-terminal edge of the β-sheet that forms their core barrel. The active site, shaped like a tunnel or pocket, is schematically divided into subsites, each one corresponding to the set of residues that interact with one monosaccharide unit of the substrate. Hence, at least two subsites are present. The subsite -1 binds the substrate glycone, *i.e.,* monosaccharide at its non-reducing end, and the subsite +1, where the substrate aglycone is positioned. GH1 β-glucosidases active upon oligocellodextrins usually have several positive subsites (+1, +2, +3 and so on) [3,4]. Residues forming the subsite -1 are conserved, whereas

Desenvolvimento Científico).The funders had no role in study design, data collection and analysis, decision to publish, or preparation of the manuscript.

Competing interests: Authors declare no conflicts of interest.

Abbreviations: Sfβgly, GH1 β-glucosidase from *Spodoptera frugiperda* (PDB 5CG0); NPβglc, *p*-nitrophenyl β-glucoside; C2, cellobiose; Tris, 2-amino-2-(hydroxymethyl)-1,3-propanediol

the positive subsites present a high variability, conferring different shapes and specificities to this active site region [2,4]. Between the subsites -1 and +1 are placed the residues involved in the hydrolysis reaction, two conserved glutamate residues that act as catalytic acid/base and nucleophile. Additionally, arginine and tyrosine residues may be present modulating the catalytic nucleophile ionization [4,5].

Tris (2-amino-2-(hydroxymethyl)-1,3-propanediol) is a buffering compound frequently employed in Biochemistry and Molecular Biology [6,7]. Its inhibitory effect was observed for aminopeptidases, amylases, and β-glucosidases [8–14]. However, there have been no efforts made to elucidate the inhibition mechanism through classical enzyme kinetics experiments.

Here we tackled that question using the recombinant GH1 β-glucosidase from *Spodoptera frugiperda* (Sfβgly). This is a digestive enzyme associated with the glycocalyx of the midgut epithelial cells from the insect *S. frugiperda*, also known as fall armyworm [15]. Sfβgly has already been characterized regarding the preference for the substrate at the subsites -1 and +1, as well as its biophysical properties such as thermal stability and dimerization [15–19].

The crystallographic structure of Sfβgly (PDB ID: 5 CG0) [17] reveals an active site comprised of two subsites. Subsite −1, which binds the monosaccharide at the non-reducing end of the substrate, is characterized by a collection of residues that form hydrogen bonds with the ligand [20]. These interactions suggest a putative binding site for small molecules that could also be involved in hydrogen bonds, like Tris. Indeed, the crystallographic structure of Sfβgly shows a Tris molecule bound into the subsite -1. This finding was unintentional and only occurred because the buffer used in the protein crystallization contained Tris [17]. However, this indicates the potential inhibitory effect of Tris on this enzyme.

Here enzyme kinetic experiments were planned to characterize the mechanism of inhibition of Sfβgly by Tris. Noteworthy, we used Tris concentrations similar to those typically used in buffers, in the mM tens range. The binding of a Tris molecule to Sfβgly was also tested using computational docking, enabling comparison between these *in silico* models and the crystallographic structure. The kinetic and structural data were combined to produce a coherent view of the interaction between Sfβgly and Tris, as well as the resulting inhibition mechanism. Finally, we discussed the possibility that Tris might affect other of GH 1 β-glucosidases. This observation should be taken into account in their study, emphasizing the importance of the appropriate buffer for accurate enzyme characterization.

2. Materials and methods

2.1. Protein preparation

Sfβgly production and purification have been previously reported [17,18]. The homogeneity of the samples was checked by SDS-PAGE [21]. Protein concentration was measured using the bicinchoninic acid (BCA) assay [22]. The purified Sfβgly sample was submitted to buffer exchange using PD Minitrap G-25 columns (Cytiva, Marlborough, MA, USA). The final sample was then stored in 100 mM phosphate buffer pH 6 at 4°C (S1 Fig).

2.2. Determination of the Sfβgly catalytic activity

The hydrolysis activity of Sfβgly upon *p*-nitrophenyl β-glucoside (NPβglc) and cellobiose (C2) was determined as previously described [23]. Initial rates were calculated from the slope of lines correlating the [product] and time. Linear regression and correlation coefficients (R^2) were used to evaluate the lines. Lines with R^2 values higher than 0.95 were accepted.

Transglycosylation reactions were detected based on the ratio of the two products, *p*-nitrophenolate, and glucose, formed from 20 mM NPβglc [23]. The *p*-nitrophenolate and glucose standard curves, prepared with and without Tris, showed no significant differences.

Substrates and Tris were prepared in 100 mM phosphate buffer pH 6. To prevent unexpected changes in the pH of the phosphate buffer, Tris was initially combined with buffering components, and only after that the pH was set to 6. NaCl was added to the phosphate buffer without Tris to adjust the ionic strength. Assays were performed at 30°C.

The effect of Tris on Sfβgly stability was assessed by incubating enzyme samples in the presence and absence of 300 mM Tris for 18 hours at 30°C. Next, Tris was removed by washing the enzyme sample with 50 volumes of 100 mM phosphate buffer pH 6. Centrifugal filter devices (Amicon Ultracel-3K, Millipore, Burlington, MA, USA) were used for this step. Finally, the enzyme activities of those samples after Tris removal were determined using 10 mM NPβglc, as mentioned above.

2.3. Inhibition of the Sfβgly activity with Tris

The initial rate of hydrolysis of 10 different substrate concentrations (NPβglc or C2) was determined in the presence of 5 different Tris concentrations (0 – 120 mM). NPβglc ranged from 0.25 to 10 mM, whereas C2 from 0.6 to 16 mM.

Initial rates were determined based on three reactions performed at 30°C. NPβglc, C2, and Tris were prepared in 100 mM phosphate buffer pH 6.0. Tris was initially combined with buffering components and only after that the pH was set to 6. Products, *p*-nitrophenolate, and glucose, were detected as previously described [23]. NaCl was added to adjust the ionic strengths among reactions, with 120 mM Tris as the reference. Experiments were performed with two different enzyme samples. Data were analyzed using Lineweaver–Burk plots. Linear fittings were accepted when showing R^2 higher than 0.9. K_i and α determination were based on procedures appropriated to the inhibition mechanism [24] and expressed as median and standard deviation.

2.4. Computational docking between Tris and GH1 β-glucosidases

GH1 β-glucosidases spatial coordinates were obtained from the PDB Data Bank. Entries were indicated in the text and figure legends. Tris coordinates were generated using Gabedit v.2.5.1 [25]. AutoDockTools 1.5.7 was used to delete water molecules, ions, and other molecules add hydrogen atoms in the protein structures, and build the grid box coordinates covering all protein atoms [26]. Dockings were performed using AutoDock Vina [27] searching the 9 best models. Tris was docked in the mono-protonated state (+1 charge). The Sfβgly-NPβglc complex coordinates were obtained by the structural alignment between the structures deposited under the PDBID 5 CG0 and 3AI0. After the alignment, a PDB file was built by retaining only the coordinates of the Sfβgly (from the 5 CG0 file) and the NPβglc (from the 3AI0 file). The Tris-enzyme complexes representing the different docking solutions were visualized by using PYMOL v0.99 software (Schrodinger LLC, NewYork, NY, USA).

3. Results and discussion

The addition of 40 mM Tris reduced to 60% the initial rate of NPβglc hydrolysis catalyzed by Sfβgly (Fig 1). However, Tris did not irreversibly inactivate Sfβgly, as pre-incubation with 300 mM Tris for 18 h did not change the reaction rate in the assays performed after Tris removal (Fig 1). Furthermore, Tris did not favor the occurrence of transglycosylation reaction catalyzed by Sfβgly given that in the presence of 30 mM Tris the ratio of glucose to *p*-nitrophenolate formation from NPβglc is 1 (Fig 1). As known, in transglycosylation reactions having NPβglc as substrate, the glucose is incorporated in the product, so that ratio should drop. Importantly standard curves for *p*-nitrophenolate and glucose prepared in the presence and absence of 120 mM Tris demonstrated that it does not affect the detection of these products (Fig 1). In short, these results suggest that Tris acts as a reversible inhibitor of Sfβgly.

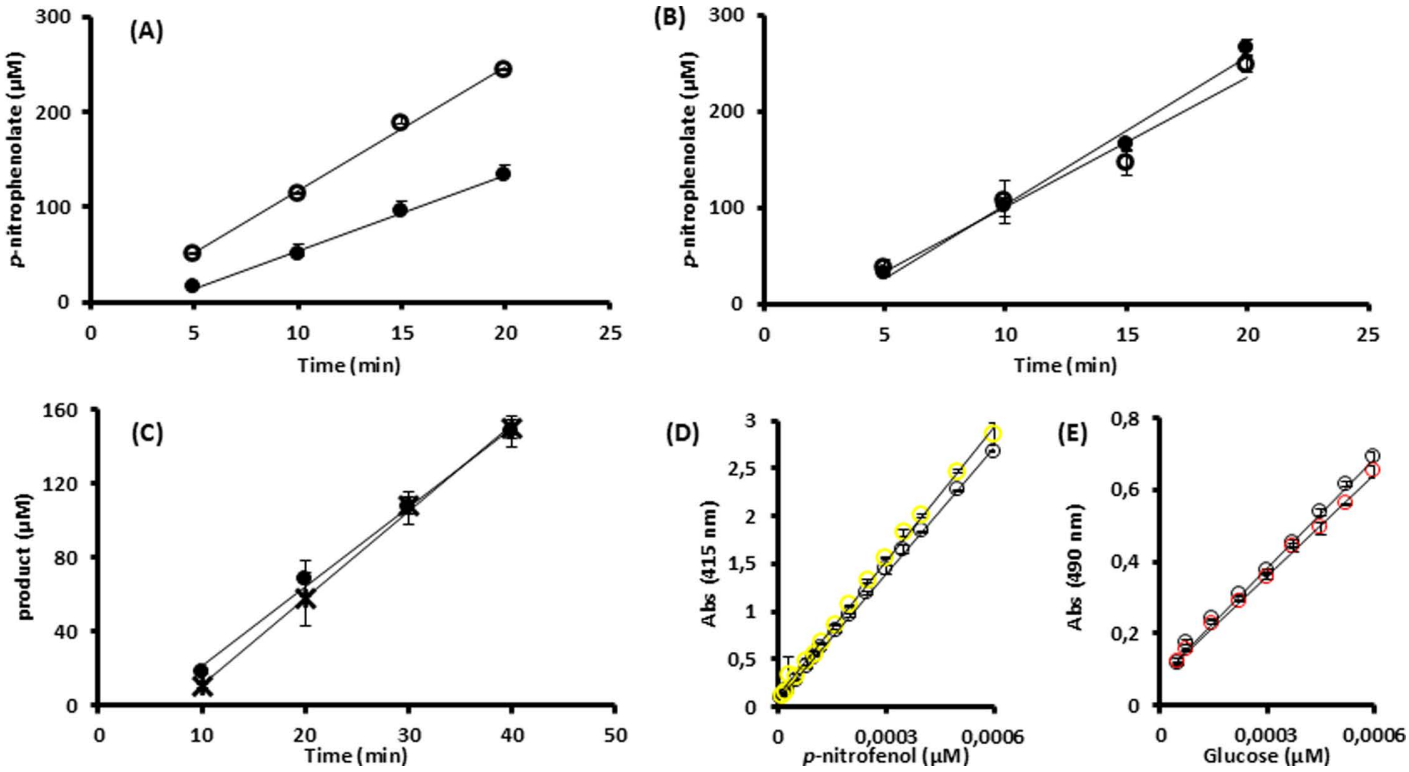

Fig 1. Effect of Tris on the Sfβgly activity and stability. (A) Initial rate of 10 mM NPβglc hydrolysis catalyzed by Sfβgly in the absence (○; 13 μM.min^{-1}) and presence of 40 mM Tris (●; 7.9 μM.min^{-1}). (B) Initial rate of 10 mM NPβglc hydrolysis catalyzed by Sfβgly previously incubated with 300 mM Tris at 30 °C for 18 **h** (●; 15 μM.min^{-1}) and without Tris (○; 13 μMmin^{-1}). Both experiments, shown in A and B, were performed with 0.09 μM Sfβgly. Data are mean and standard deviation of three determinations of the product formed in each incubation time using three separate assays with the same enzyme sample. The substrate was prepared in 100 mM phosphate buffer pH 6.0. Activity assays were performed at 30 °C. (C) Tests aiming at the detection of the transglycosylation reaction catalyzed by Sfβgly (0.009 μM). Production of *p*-nitrophenolate (○) and glucose (*) from 20 mM NPβglc in the presence of 30 mM Tris. The substrate was prepared in 100 mM phosphate buffer pH 6.0. Activity assays were done at 30 °C. Data are mean and standard deviation of three determinations of the product formed in each incubation time using the same enzyme sample. (D) Standard curve of *p*-nitrophenolate with (○) and without (○) 120 mM Tris. Slopes are 4420 and 4721 Abs_{415nm}. μM^{-1}, respectively. (E) Standard curve of glucose with (○) and without (○) 120 mM Tris. Slopes are 1007 and 935 Abs_{415nm}. μM^{-1}, respectively. R^2 are higher than 0.99.

https://doi.org/10.1371/journal.pone.0320120.g001

To uncover the mechanism of that inhibition, the initial hydrolysis rate of various NPβglc concentrations determined at different Tris concentrations were analyzed using Lineweaver-Burk plots. The experiment was performed three times with two independent enzyme samples (S1 Fig), producing the same pattern (Fig 2; S2 and S3 Figs). Increments of Tris concentration generated a set of lines with increasing K_s/k_3 (slope) and $1/k_3$ (intercept). In addition, those lines intersected above the 1/[S] axis in the second quadrant. Finally, the apparent K_s/k_3 and apparent $1/k_3$ showed a linear relation with the Tris concentration (Fig 2; S2 and S3 Figs). These features define a linear mixed-type inhibition mechanism, specifically an intersecting, linear, noncompetitive inhibition (Fig 2) [24].

A linear mixed-type inhibition mechanism indicates that Tris (inhibitor) and NPβglc (substrate) may both bind to the Sfβgly enzyme, forming a non-productive complex ESI. So even in the presence of a theoretical infinite substrate concentration, which should result in the limiting initial rate (V_{max}), the presence of Tris would drive a fraction of the enzyme population to be locked in the inactive ESI complex. Hence, a lower apparent V_{max} is reached in the presence of Tris. As a result, the line intercept, *i.e.,* $1/k_3$ which is proportional to $1/V_{max}$, (Fig 2; S2 and S3 Figs) increases with increasing Tris concentration.

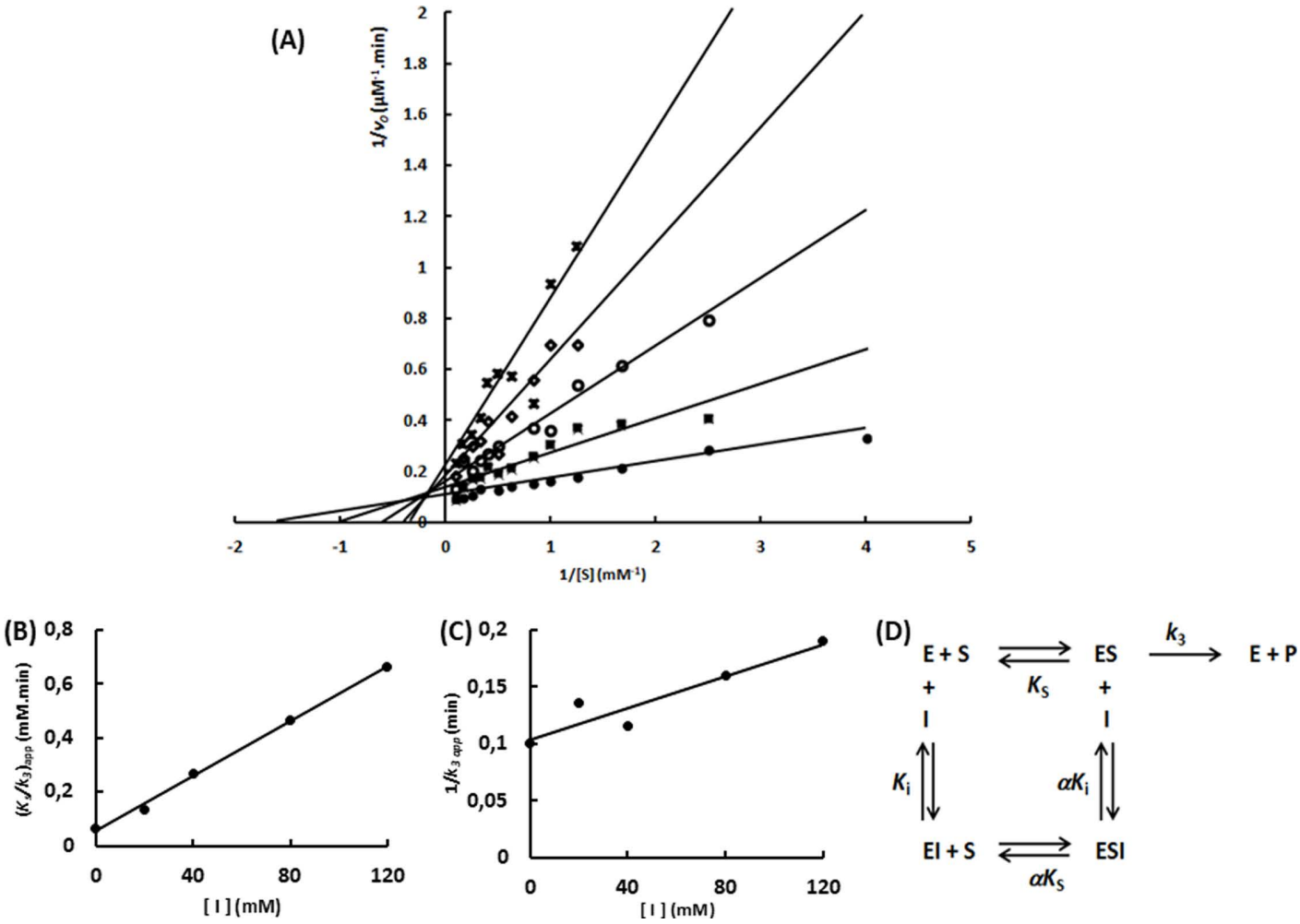

Fig 2. Characterization of the Tris inhibition mechanism upon Sfβgly. (A) Lineweaver-Burk plots showing the effect of different Tris concentrations (●, 0; ▪, 20 mM; ○, 40 mM; ◊, 80 mM; x, 120 mM) on the initial rate of hydrolysis of the substrate NPβglc. (B) Tris effect on the apparent K_s/k_3 (calculated from the line slope). (C) Tris effect on the apparent 1/ k_3 (calculated from the line intercept). NPβglc and Tris were prepared in 100 mM phosphate buffer pH 6.0. Rates were determined at 30°C. Rates are the mean of three product determinations using the same enzyme sample. Experiment performed with enzyme sample #1. Independent experiments were performed using two different enzyme samples (S1 and S2 Figs). (D) Linear mixed-type inhibition mechanism (intersecting, linear, noncompetitive). S, substrate NPβglc; I, inhibitor Tris; E, enzyme Sfβgly; P, product; K_s, dissociation constant for the ES complex; K_i, dissociation constant for the EI complex; k_3, rate constant for product formation; α, factor that represents the mutual hindering effect between S and I (α > 1) [24].

https://doi.org/10.1371/journal.pone.0320120.g002

Besides that, both the inhibitor Tris and the substrate NPβglc, can bind to the free enzyme and the ES complex (Fig 2). However, the presence of one ligand, substrate, or inhibitor, hampers the binding of the second one. Hence, the affinity between the substrate and EI complex is lower than that between substrate and E, whereas the inhibitor affinity for the ES complex is also lower than for E. Therefore, αK_i and αK_s are higher than K_i and K_s, respectively. Consequently, the factor α, that is higher than 1, represents the detrimental effect that the first ligand (substrate or Tris) exerts upon the second ligand binding.

The same experiment was repeated using C2, a natural substrate of Sfβgly, and two independent enzyme samples. The same inhibitory mechanism was observed (Fig 3; S4 Fig).

Then, considering that Tris was shown to be a linear mixed-type inhibitor of Sfβgly, the apparent K_s/k_3 *versus* [Tris] and apparent $1/k_3$ *versus* [Tris] (Fig 2; Fig 3; S2–S4 Figs) plots were employed to calculate the K_i and α(Table 1) [24].

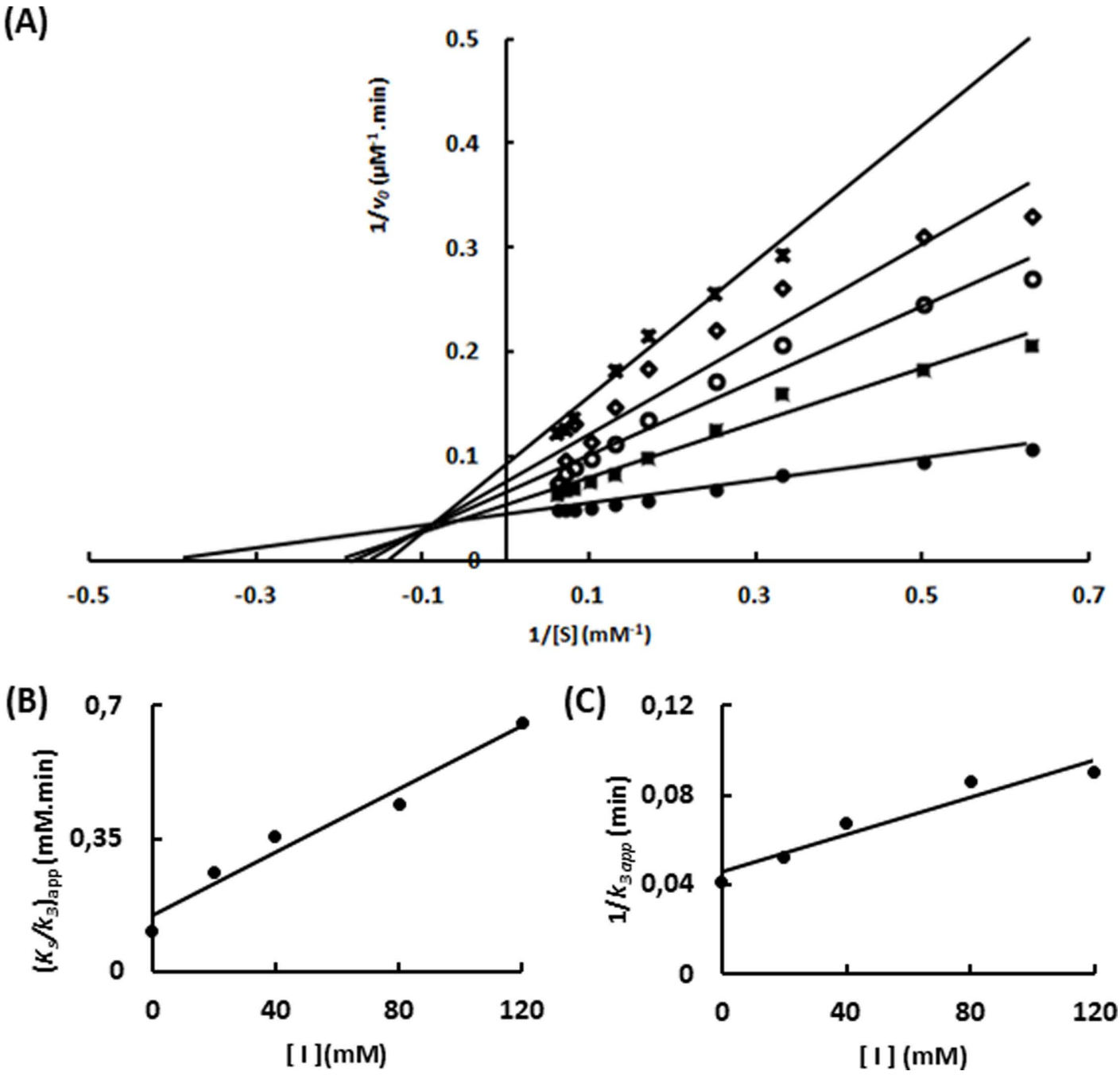

Fig 3. Characterization of the Tris inhibition mechanism upon hydrolysis of the substrate C2 catalyzed by Sfβgly. (A) Lineweaver-Burk plots showing the effect of different Tris concentrations ●, 0; ▪, 20 mM; ○, 40 mM; ◊, 80 mM; x, 120 mM) on the initial rate of C2 hydrolysis. (B) Tris effect on the apparent K_s/k_3 (calculated from the line slope). (C) Tris effect on the apparent $1/k_3$ (calculated from the line intercept). C2 and Tris were prepared in 100 mM phosphate buffer pH 6.0. Rates were determined at 30°C. Rates are the mean of three product determinations using the same enzyme sample. Two independent experiments were performed using two different enzyme samples (S4 Fig).

https://doi.org/10.1371/journal.pone.0320120.g003

The inhibition mechanism is shown in Fig 2. K_i represents the dissociation constant of the Sfβgly enzyme-Tris complex (EI). α corresponds to the mutual hindering effect involving substrate and Tris. Data are averages and standard deviations. n = 2 for C2 and n = 3 for NPβglc.

Table 1. Parameters of the Tris inhibition mechanism upon the β-glucosidase Sfβgly.

Substrate	K_i (mM)	α
C2	35.5 ± 0.7	2.7 ± 0.7
NPβglc	12 ± 2	3 ± 1

https://doi.org/10.1371/journal.pone.0320120.t001

The similar K_i observed with two different substrates suggests that Tris is binding in the same site in both cases. The factor $\alpha > 1$ confirms a significant mutual impediment involving Tris and the substrate, showing that the first ligand causes a 3-fold decrease in the affinity of the second one. The physical nature of this effect is not clear by now, but a steric hindrance resulting in an alteration of the distances and angles of the non-covalent interactions involved in the substrate or inhibitor binding could be proposed.

Thus, the previous suggestion of non-specific binding of Tris to Sfβgly implying no inhibitory effect [28] was not supported by the results presented here. On the other hand, the linear mixed-type inhibition mechanism contrasts to the competitive mechanism proposed for *Rhynchoschiara americana*, *Thermoanaerobacterium saccharolyticum*, *Oryza sativa,* and *Acidilobus Saccharovorans* β-glucosidases [13,14,29–31]. Finally, in addition to extending the observations of the Tris inhibitory effect on β-glucosidases [10–14,28–31], the detailed mechanism presented here (Fig 2) can be compared with the structural information available to compose a more comprehensive picture.

Indeed, Tris had been previously observed in the Sfβgly crystallographic structure within the enzyme active site (S5 Fig; 5 CG0). The presence of additional Tris binding sites in the Sfβgly, which could be compatible with the inhibition mechanism (Fig 2), was searched by computational docking. Nevertheless, this approach also revealed a set of similarly possible binding sites (S1 Table; S6 Fig) within the active site encircled (distance ≤ 3.5 Å) by the subsite -1 residues Y331, W444, and E451 and around the catalytic residues E187 and E399 (Fig 4A) [5,15,16,17,20]. In short, the crystallographic structure and the molecular docking showed the same binding mode for Tris and Sfβgly. Tris interaction within the -1 subsite had been previously reported for GH 1 β-glucosidases (PDB ID: 3GNO, 3AHZ, 3AHY, 3W53, 4MDO, 4RE2, 7E5J, and 8PUO) [10,14,28,32].

But this binding mode (Fig 4A), *i.e.* within the active site, is not compatible with the mixed inhibitory mechanism observed here (Fig 2). Actually, it would be consistent with a simple competitive inhibition [24], as suggested before [13,14,29–31].

Hence in a complementary approach to search for alternative Tris binding sites, the Sfβgly-NPβglc complex (ES) was employed in the molecular docking (S2 Table; S7 Fig), revealing a solution in which a Tris molecule is placed in a lateral pocket in the active site opening, surrounded by (distance ≤ 3.5 Å) residues R189, F251, R267, E271 and S358 (Fig 4B). Imidazole had been previously found to inhibit Sfβgly by interacting in that same region [23]. Hence, Tris positioning in such a pocket could be compatible with the simultaneous binding of the substrate in the -1 and +1 subsites. However, their simultaneous presence could misplace the substrate relatively to the catalytic residues, which would produce a non-productive ESI complex. In short, this Tris docking solution is compatible with a linear mixed-type inhibition (Figs 2 and 4B).

The potential of pockets around the active site opening, as this suggested for Tris, as a binding site for small ligands was strengthened by inspection of the crystallographic data of several GH1 β-glucosidases (PDB ID: 3GNO from *Oryza sativa*, 4MDO from *Humicola insolens*, 4RE2, and 4RE3 also from *Oryza sativa*). Those β-glucosidase structures show ligands simultaneously occupying their active site and pockets around the active site entrance. The structural alignment between these enzymes and the Sfβgly-NPβglc-Tris complex revealed that small ligands such as glycerol (PDB ID: GOL), di(hydroxyethyl)ether (PEG)

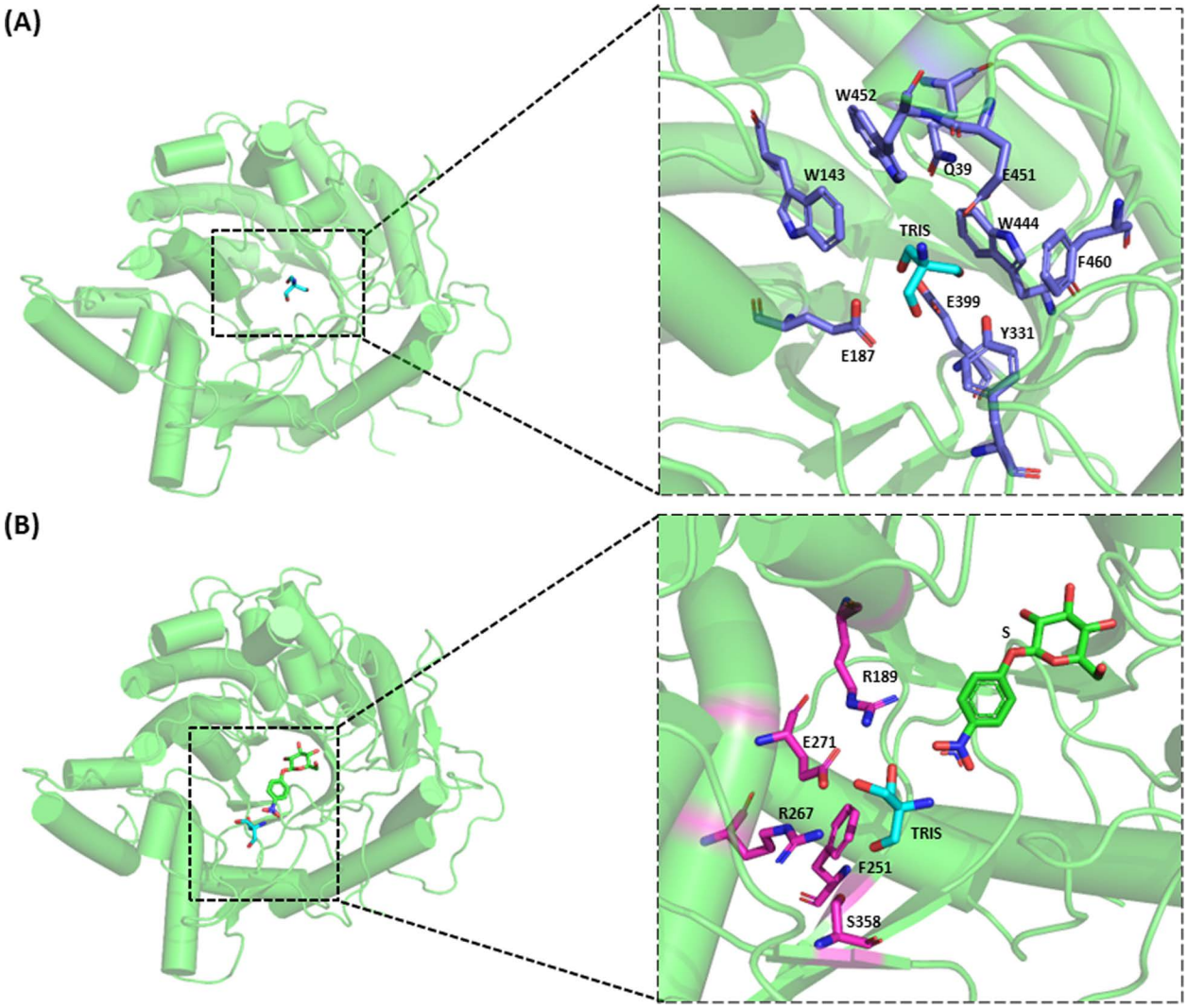

Fig 4. Tris binding in the β-glucosidase Sfβgly and the Sfβgly-NPβglc complex. (A) Binding spots in the free enzyme revealed by computational docking (solutions #1 to #7 – S1 Table; S6 Fig). Residues interacting with Tris are shown in blue. (B) Binding spots in the enzyme-substrate complex revealed by computational docking (S2 Table; S7 Fig) Residues showed in the detailed structures (panels A and B) are within 3.5 Å of the Tris molecule.

https://doi.org/10.1371/journal.pone.0320120.g004

and hydroxyethyl piperazine ethanesulfonic acid (PDB ID: EPE) are found around the same binding pocket occupied by Tris (Fig 4B; S8 Fig). In short, the presence of inhibitor binding sites beyond the active site in GH1 β-glucosidases was revealed by the molecular docking and crystallographic structures.

The observation of two putative binding sites for Tris in the Sfβgly (Fig 4A and Fig 4B) is not incoherent since Tris has multiple groups that could be involved in hydrogen bonds (3 hydroxyls and 1 amine) with the many polar residues along the active site tunnel, which usually interact with the hydroxyl groups of the Sfβgly natural substrates, *i.e.,* oligocellodextrins [5,16,20].

As a final support to the presence of a Tris binding pocket in the opening of the Sfβgly active site (Fig 4B), the superimposition of the chains A to F of its crystallographic structure (PDB ID 5 CG0) showed a total of six water molecules (867 and 1033 from chain A, 955 from chain C, 783 and 841 from chain E and 739 from chain F) surrounded by the same residues (R189, F251, R267, E271 and S358; distance ≤ 3.5 Å) that interact with Tris in the active site opening (Fig 4B; S9 Fig). Curiously,

the positioning of the O atoms of those water molecules is similar (deviation ≤ 1 Å) to the N1, C1, C3, O2, and O3 atoms of the Tris molecule (S9 Fig). Besides that, the distance between the O atom from H_2O 867 and 783 and the side chains of E271 (O_δ) and S358 (O_β) (2.97 and 2.72 Å, respectively) are similar to the distances of the hydrogen bonds connecting the side chains of E271 and S358 to the Tris O3 and O2 (3.12 and 3.17 Å, respectively). Hence, the Tris binding pocket in the opening of the Sfβgly active site has indeed potential to interact with polar ligands.

Therefore, the Tris docking solution depicted in Fig 4B, which allows the simultaneous binding of the substrate and Tris, could generate the linear mixed inhibition mechanism observed here (Fig 2).

Based on this, it could be anticipated that small molecules presenting hydrogen bond potential (for instance Tris, imidazole, glycerol, and so on) may find binding spots around the active site entrance of the GH1 β-glucosidases. Computational docking of Tris into several GH1 β-glucosidases points in that direction (S10 Fig). Interestingly, as also previously noted [14,28], Tris interaction within the subsite -1 and the shape variability of β-glucosidases active site, particularly in the more external portions that probably constitute the positive subsites and opening, suggests a multiplicity of possible binding modes, which could produce contrasting inhibition mechanisms for different β-glucosidases. Thus, as previously observed [13,14,28,29] and here detailed, Tris inhibition probably also affects other GH1 β-glucosidase. This observation should be considered in the study of these enzymes, stressing the importance of the appropriate buffer for their accurate characterization.

Supporting information

S1 Fig. SDS-PAGE of the purified recombinant Sfβgly.
(TIF)

S2 Fig. Characterization of the Tris inhibition mechanism upon Sfβgly. Enzyme sample #1. Substrate NPβglc.
(TIF)

S3 Fig. Characterization of the Tris inhibition mechanism upon Sfβgly. Enzyme sample #2. Substrate NPβglc.
(TIF)

S4 Fig. Characterization of the Tris inhibition mechanism upon Sfβgly. Enzyme sample #2. Substrate C2.
(TIF)

S1 Table. Docking solutions for Tris binding in the GH1 β-glucosidase Sfβgly.
(TIF)

S2 Table. Docking solutions for Tris binding in the Sfβgly-NPβglc complex.
(TIF)

S5 Fig. Tris bound within the Sfβgly active site. Based on PDB 5 CG0.
(TIF)

S6 Fig. Mapping of the docking solutions for Tris binding in the GH1 β-glucosidase Sfβgly.
(TIF)

S7 Fig. Mapping of the docking solutions for Tris binding in the Sfβgly-NPβglc complex.
(TIF)

S8 Fig. Small ligands binding pockets in the active site opening of GH1 β-glucosidases.
(TIF)

S9 Fig. Comparison of the Tris and H_2O binding in the opening of the Sfβgly active site.
(TIF)

S10 Fig. Docking solutions for Tris binding in the active site of different GH1 β-glucosidases.
(TIF)

Author contributions

Conceptualization: Rafael Siqueira Chagas, Sandro R. Marana.

Formal analysis: Rafael Siqueira Chagas, Sandro R. Marana.

Funding acquisition: Sandro R. Marana.

Investigation: Rafael Siqueira Chagas, Sandro R. Marana.

Resources: Sandro R. Marana.

Writing – original draft: Rafael Siqueira Chagas, Sandro R. Marana.

Writing – review & editing: Rafael Siqueira Chagas, Sandro R. Marana.

References

1. Drula E, Garron M-L, Dogan S, Lombard V, Henrissat B, Terrapon N. The carbohydrate-active enzyme database: functions and literature. Nucleic Acids Res. 2022;50(D1):D571–7. https://doi.org/10.1093/nar/gkab1045 PMID: 34850161
2. Ketudat Cairns JR, Esen A. β-Glucosidases. Cell Mol Life Sci. 2010;67(20):3389–405. https://doi.org/10.1007/s00018-010-0399-2 PMID: 20490603
3. Davies G, Henrissat B. Structures and mechanisms of glycosyl hydrolases. Structure. 1995;3(9):853–9. https://doi.org/10.1016/S0969-2126(01)00220-9 PMID: 8535779
4. Marana SR. Molecular basis of substrate specificity in family 1 glycoside hydrolases. IUBMB Life. 2006;58(2):63–73. https://doi.org/10.1080/15216540600617156 PMID: 16611572
5. Marana SR, Mendonça LMF, Andrade EHP, Terra WR, Ferreira C. The role of residues R97 and Y331 in modulating the pH optimum of an insect beta-glycosidase of family 1. Eur J Biochem. 2003;270(24):4866–75. https://doi.org/10.1046/j.1432-1033.2003.03887.x PMID: 14653813
6. Durst RA, Staples BR. Tris-tris-HCl: a standard buffer for use in the physiologic pH range. Clin Chem. 1972;18(3):206–8. PMID: 5020814
7. Bleich HL, Schwartz WB. Tris buffer (THAM). An appraisal of its physiologic effects and clinical usefulness. N Engl J Med. 1966;274(14):782–7. https://doi.org/10.1056/NEJM196604072741407 PMID: 17926886
8. Desmarais WT, Bienvenue DL, Bzymek KP, Holz RC, Petsko GA, Ringe D. The 1.20 A resolution crystal structure of the aminopeptidase from Aeromonas proteolytica complexed with tris: a tale of buffer inhibition. Structure. 2002;10(8):1063–72. https://doi.org/10.1016/s0969-2126(02)00810-9 PMID: 12176384
9. Ghalanbor Z, Ghaemi N, Marashi S-A, Amanlou M, Habibi-Rezaei M, Khajeh K, et al. Binding of Tris to Bacillus licheniformis alpha-amylase can affect its starch hydrolysis activity. Protein Pept Lett. 2008;15(2):212–4. https://doi.org/10.2174/092986608783489616 PMID: 18289113
10. Jeng W-Y, Wang N-C, Lin M-H, Lin C-T, Liaw Y-C, Chang W-J, et al. Structural and functional analysis of three β-glucosidases from bacterium Clostridium cellulovorans, fungus Trichoderma reesei and termite Neotermes koshunensis. J Struct Biol. 2011;173(1):46–56. https://doi.org/10.1016/j.jsb.2010.07.008 PMID: 20682343
11. Ait N, Creuzet N, Cattaneo J. Properties of β-glucosidase purified from *Clostridium thermocellum*. Microbiology. 1982;128:569–577. https://doi.org/10.1099/00221287-128-3-569
12. Park SY, Bae EA, Sung JH, Lee SK, Kim DH. Purification and characterization of ginsenoside Rb1-metabolizing beta-glucosidase from Fusobacterium K-60, a human intestinal anaerobic bacterium. Biosci Biotechnol Biochem. 2001;65(5):1163–9. https://doi.org/10.1271/bbb.65.1163 PMID: 11440132

13. Ferreira C, Terra WR. Physical and kinetic properties of a plasma-membrane-bound beta-D-glucosidase (cellobiase) from midgut cells of an insect (Rhynchosciara americana larva). Biochem J. 1983;213(1):43–51. https://doi.org/10.1042/bj2130043 PMID: 6412680

14. Kim IJ, Bornscheuer UT, Nam KH. Biochemical and Structural Analysis of a Glucose-Tolerant β-Glucosidase from the Hemicellulose-Degrading Thermoanaerobacterium saccharolyticum. Molecules. 2022;27(1):290. https://doi.org/10.3390/molecules27010290 PMID: 35011521

15. Marana SR, Jacobs-Lorena M, Terra WR, Ferreira C. Amino acid residues involved in substrate binding and catalysis in an insect digestive beta-glycosidase. Biochim Biophys Acta. 2001;1545(1–2):41–52. https://doi.org/10.1016/s0167-4838(00)00260-0 PMID: 11342030

16. Mendonça LMF, Marana SR. Single mutations outside the active site affect the substrate specificity in a β-glycosidase. Biochim Biophys Acta. 2011;1814(12):1616–23. https://doi.org/10.1016/j.bbapap.2011.08.012 PMID: 21920467

17. Tamaki FK, Souza DR, Souza VP, Ikegami CM, Farah CS, Marana SR. Using the amino acid network to modulate the hydrolytic activity of β-glycosidases. PlosONE. 2016;11:1616-1623, https://doi.org/10.1016/j.bbapap.2011.08.012

18. Souza VP, Ikegami CM, Arantes GM, Marana SR. Protein thermal denaturation is modulated by central residues in the protein structure network. FEBS J. 2016;283(6):1124–38. https://doi.org/10.1111/febs.13659 PMID: 26785700

19. Otsuka FAM, Chagas RS, Almeida VM, Marana SR. Homodimerization of a glycoside hydrolase family GH1 β-glucosidase suggests distinct activity of enzyme different states. Protein Sci. 2020;29(9):1879–89. https://doi.org/10.1002/pro.3908 PMID: 32597558

20. Marana SR, Terra WR, Ferreira C. The role of amino-acid residues Q39 and E451 in the determination of substrate specificity of the Spodoptera frugiperdaβ-glycosidase. European Journal of Biochemistry. 2002;269(15):3705–14. https://doi.org/10.1046/j.1432-1033.2002.03061.x

21. Laemmli UK. Cleavage of structural proteins during the assembly of the head of bacteriophage T4. Nature. 1970;227(5259):680–5. https://doi.org/10.1038/227680a0 PMID: 5432063

22. Smith PK, Krohn RI, Hermanson GT, Mallia AK, Gartner FH, Provenzano MD, et al. Measurement of protein using bicinchoninic acid. Anal Biochem. 1985;150(1):76–85. https://doi.org/10.1016/0003-2697(85)90442-7 PMID: 3843705

23. Chagas RS, Otsuka FAM, Pineda MAR, Salinas RK, Marana SR. Mechanism of imidazole inhibition of a GH1 β-glucosidase. FEBS Open Bio. 2023;13(5):912–25. https://doi.org/10.1002/2211-5463.13595 PMID: 36906930

24. Segel IH. Enzyme Kinetics: Behavior and Analysis of Rapid Equilibrium and Steady-State Enzyme Systems. John Wiley & Sons (1993), New York, NY.

25. Allouche A-R. Gabedit--a graphical user interface for computational chemistry softwares. J Comput Chem. 2011;32(1):174–82. https://doi.org/10.1002/jcc.21600 PMID: 20607691

26. Morris GM, Huey R, Lindstrom W, Sanner MF, Belew RK, Goodsell DS, et al. AutoDock4 and AutoDockTools4: Automated docking with selective receptor flexibility. J Comput Chem. 2009;30(16):2785–91. https://doi.org/10.1002/jcc.21256 PMID: 19399780

27. Trott O, Olson AJ. AutoDock Vina: improving the speed and accuracy of docking with a new scoring function, efficient optimization, and multithreading. J Comput Chem. 2010;31(2):455–61. https://doi.org/10.1002/jcc.21334 PMID: 19499576

28. Nam KH. Structural analysis of Tris binding in β-glucosidases. Biochem Biophys Res Commun. 2024;700:149608. https://doi.org/10.1016/j.bbrc.2024.149608 PMID: 38306932

29. Trofimov AA, Polyakov KM, Tikhonov AV, Bezsudnova EY, Dorovatovskii PV, Gumerov VM, et al. Structures of β-glycosidase from acidilobus saccharovorans in complexes with tris and glycerol. Dokl Biochem Biophys. 2013;449:99–101. https://doi.org/10.1134/S1607672913020129 PMID: 23657657

30. Sansenya S, Opassiri R, Kuaprasert B, Chen C-J, Cairns JRK. The crystal structure of rice (Oryza sativa L.) Os4BGlu12, an oligosaccharide and tuberonic acid glucoside-hydrolyzing β-glucosidase with significant thioglucohydrolase activity. Arch Biochem Biophys. 2011;510(1):62–72. https://doi.org/10.1016/j.abb.2011.04.005 PMID: 21521631

31. Seshadri S, Akiyama T, Opassiri R, Kuaprasert B, Cairns JK. Structural and enzymatic characterization of Os3BGlu6, a rice beta-glucosidase hydrolyzing hydrophobic glycosides and (1->3)- and (1->2)-linked disaccharides. Plant Physiol. 2009;151(1):47–58. https://doi.org/10.1104/pp.109.139436 PMID: 19587102

32. Gourlay LJ, Mangiagalli M, Moroni E, Lotti M, Nardini M. Structural determinants of cold activity and glucose tolerance of a family 1 glycoside hydrolase (GH1) from Antarctic Marinomonas sp. ef1. FEBS J. 2024;291(13):2897–917. https://doi.org/10.1111/febs.17096 PMID: 38400529